Accelerating CO2 Dissolution in Saline Aquifers for Geological Storage — Mechanistic and Sensitivity Studies

ARTICLE *in* ENERGY & FUELS · JUNE 2009

Impact Factor: 2.79 · DOI: 10.1021/ef900125m

3 AUTHORS, INCLUDING:

Hassan Hassanzadeh
The University of Calgary
74 PUBLICATIONS **573** CITATIONS

SEE PROFILE

David Keith
Harvard University
154 PUBLICATIONS **5,143** CITATIONS

SEE PROFILE

Accelerating CO_2 Dissolution in Saline Aquifers for Geological Storage − Mechanistic and Sensitivity Studies

Hassan Hassanzadeh, Mehran Pooladi-Darvish,* and David W. Keith

Department of Chemical and Petroleum Engineering, Schulich School of Engineering, University of Calgary, 2500 University Drive NW, Calgary, AB Canada, T2N 1N4

Received February 12, 2009. Revised Manuscript Received April 9, 2009

One of the important challenges in geological storage of CO_2 is predicting, monitoring, and managing the risk of leakage from natural and artificial pathways such as fractures, faults, and abandoned wells. The risk of leakage arises from the buoyancy of free-phase mobile CO_2 (gas or supercritical fluid). When CO_2 dissolves into formation brine, or is trapped as residual phase, buoyancy forces are negligible and the CO_2 may be retained with minimal risk of leakage. Solubility trapping may therefore enable more secure storage in aquifer systems than is possible in dry systems (e.g., depleted gas fields) with comparable geological seals. A crucial question for an aquifer system is, what is the rate of dissolution? In this paper, we address that question by presenting a method for accelerating CO_2 dissolution in saline aquifers by injecting brine on top of the injected CO_2. We investigate the effects of different aquifer properties and determine the rate of solubility trapping in an idealized aquifer geometry. The acceleration of dissolution by brine injection increases the rate of solubility trapping in saline aquifers and therefore increases the security of storage. We show that, without brine injection, only a small fraction (less than 8%) of the injected CO_2 would be trapped by dissolving in formation brine within 200 years. For the particular cases studied, however, more than 50% of the injected CO_2 dissolves in the aquifer as induced by brine injection. Since the energy cost for brine injection can be small (<20%) compared to the energy required for CO_2 compression for a 5-fold increase in dissolution, such reservoir engineering techniques might be viable and practical for accelerating dissolution of CO_2. The environmental benefit would be to decrease the risk of CO_2 leakage at reasonably low cost.

1. Introduction

CO_2 storage in saline aquifers has been treated in the literature since the early 1990s.[1] At least three alternatives have been suggested for geological CO_2 storage. These include: depleted oil and gas reservoirs, deep saline aquifers, and coal seams.[2] In aquifers, storage may occur by several mechanisms: injected CO_2 dissolves in the formation water (solubility trapping),[3] some may be trapped as residual phase saturation (residual phase trapping),[4,5] and some may react with host minerals to precipitate carbonates (mineral trapping).[6−8] In this work, we focus on the solubility trapping of CO_2 in saline formations and investigate the possibility of accelerating the process by existing reservoir engineering practices.

The CO_2 injected into a saline aquifer is less dense than the resident brines. Driven by density contrasts, CO_2 will flow horizontally (in a horizontal aquifer), spreading under the cap rock, and potentially will flow upward given the availability of leaks through any high-permeability zones or artificial penetrations such as abandoned wells. The mobile free-phase CO_2 (gas or supercritical fluid) slowly dissolves in the formation brines. Free convective mixing[9−16] and mineral trapping[6−8] contribute to CO_2 trapping, but the time-scales for such processes are typically long.

Assessments of the risk of leakage of CO_2 from storage formations may need to consider leakage mechanisms and their likelihood of occurrence during the full time period over which mobile free-phase CO_2 is expected to remain in the reservoir. Once dissolved, risk assessments may well ignore the leakage pathways, owing to the very slow movement of CO_2-saturated brines. If it were practical to accelerate the dissolution of CO_2 in brines, one could reduce the time-scale in which leakage is

* Corresponding author. Phone: (403) 220-8779; fax (403)284-4852; e-mail: pooladi@ucalgary.ca.

(1) Intergovernmental Panel on Climate Change (IPCC). *Special Report on Carbon Dioxide Capture and Storage*; Cambridge University Press: **2005**.
(2) Gale, J. *Energy.* **2004**, 291329–1338.
(3) Bachu, S.; Adams, J. J. *Energy Convers. Manage.* **2003**, *44* (20), 3151–3175.
(4) Kumar, A.; Ozah, R.; Noh, M.; Pope, G. A.; Bryant, S.; Sepehrnoori, K.; Lake, L. W.; Noh, M.; Pope, G. A.; Bryant, S.; Sepehrnoori, K.; Lake, L. W. *Soc. Pet. Eng. J.* **2003**, *10* (3), 336–348.
(5) Juanes, R.; Spiteri, E. J.; Orr, F. M., Jr.; Blunt, M. J. *Water Resour. Res.* **2006**, 42.
(6) Bachu, S.; Gunter, W. D.; Perkins, E. H. *Energy Convers. Manage.* **1994**, *35* (4), 269–279.
(7) Gunter, W. E.; Perkins, E. H.; Wiwchar, B. *Mineral. Petrol.* **1997**, *59*, 121–140.
(8) Pruess, K.; Xu, T.; Apps, J.; García, J. *Soc. Pet. Eng. J.* **2003**, 49–60.
(9) Lindeberg, E. G. B.; Wessel-Berg, D. *Energy Convers. Manage.* **1996**, *38 S*, 229–234.
(10) Ennis-King, J.; Preston, I.; Paterson, L. *Phys. Fluids.* **2005**, *17* (8), 084107.
(11) Hassanzadeh, H.; Pooladi-Darvish, M.; Keith, D. *J. Can. Pet. Technol.* **2005**, *44* (10), 43–51.
(12) Ennis-King, J.; Paterson, L. *Soc. Pet. Eng. J.* **2005**, *10* (3), 349–356.
(13) Riaz, A.; Hesse, M.; Tchelepi, A.; Orr, F. M., Jr. *J. Fluid Mech.* **2006**, *548*, 87–111.
(14) Xu, X.; Chen, S.; Zhang, D. *Adv. Water Resour.* **2006**, *29*, 397–407.
(15) Hassanzadeh, H.; Pooladi-Darvish, M.; Keith, D. *Transport Porous.* **2006**, *65* (2), 193–211.
(16) Hassanzadeh, H.; Pooladi-Darvish, M.; Keith, D. *AIChE J.* **2007**, *53* (5), 1121–1131.

10.1021/ef900125m CCC: $40.75
Published on Web 04/29/2009

possible, reducing the risks of leakage and thereby simplifying risk assessments.

In this study, a commercial black-oil reservoir simulator[17] is used to investigate the effect of brine injection on accelerating CO_2 dissolution into formation brines using an idealized 2D radial geometry for the aquifer and brine injection well. Subsequent to the completion of this work, Leonenko and Keith[18] have recently investigated the role of reservoir geometry on accelerating CO_2 dissolution. In this paper, the effects of a number of other reservoir engineering parameters that may affect the CO_2 solubility trapping are studied. These parameters include aquifer layering, permeability anisotropy, and aquifer tilt angle. In addition, an engineering design is presented for accelerating CO_2 dissolution in a saline aquifer by brine injection on top of the injected CO_2 plume. The outline of the paper is as follows. First, we briefly review the previous reservoir simulation studies on aquifer storage of CO_2, which are closely related to this study. Discussion of the reservoir and fluid models follows. Next, results of the reservoir simulation studies are discussed and conclusions are presented.

2. Previous Work

As mentioned by van der Meer in the early investigations on numerical simulation of CO_2 storage in saline aquifers, the dominant short-term processes that determine dissolution rates are gravity segregation and viscous displacement, and as altered by viscous fingering and formation heterogeneity.[19−22] Holt et al.[23] conducted reservoir simulation studies to investigate the storage capacity defined as CO_2 dissolved in formation brine. For the cases studied, CO_2 storage capacity varied between 13 and 26% of pore volume. Using reservoir simulation, Law and Bachu[24] showed that a similar fraction of CO_2 may dissolve into the brine and travel within the slow hydrodynamic system in the aquifer. Refined numerical simulations presented in this study show dissolution values less than 8% without brine injection. Ennis-King et al.[25] simulated the long-term geological storage of CO_2 in a detailed geological model. They also mentioned that use of coarse grids would lead to overestimation of dissolution rate during the injection period. In a code comparison study, Pruess et al.[26,27] also identified some discrepancies between different simulators, claiming that such are related to differences in fluid property correlations and space and time discretizations. In addition, Pruess et al.[8] studied CO_2 storage in saline aquifers and found that the long-term total storage capacity could be on the order of 30 kg/m^3 of aquifer volume for all trapping mechanisms. Flett et al.[28] investigated the impact of heterogeneity on containment and trapping of carbon dioxide in saline formations.

Besides naturally occurring trapping mechanisms such as solubility, residual phase, and mineral trapping discussed above, reservoir engineering techniques may also be used to accelerate CO_2 dissolution in saline aquifers. In such methods, formation brine can be produced from a far distant location and injected back on top of the injected CO_2 plume. Keith et al.[29] and Leonenko et al.[30] investigated the role of brine injection on top of a CO_2 plume for accelerating CO_2 dissolution in formation brines. They found that such a technique could improve CO_2 dissolution significantly. They concluded that reservoir engineering techniques might be used to increase storage efficiencies and could decrease the risk of leakage at comparatively low cost.

Our objective in this work is to extend the previous studies[18,29,30] and use current black-oil reservoir simulation technology to perform more comprehensive numerical simulations for investigating the role of brine injection on top of a CO_2 plume, leading to accelerated solubility trapping mechanisms. In this study, an engineering design is presented to accelerate CO_2 dissolution in formation brines. It is shown that brine injection can potentially accelerate the CO_2 dissolution in saline aquifers and therefore reduce the time-scale in which there is a chance of CO_2 leakage. It is shown that the energy costs for brine injection can be small compared to that of CO_2 capture and compression costs. The CO_2 emissions from operating the brine injector can, for example, be less than 2% of the amount of CO_2 in storage. In addition, effects of various aquifer parameters have been studied. Such reservoir engineering techniques are demonstrated to be possible for accelerating the rate of solubility trapping of CO_2, thereby decreasing the risk of leakage at reasonably low cost.

3. Representation of CO_2−Brine Equations of State Predictions in a "Black-oil" Simulator

The choice of fluid model is very important in simulating CO_2 storage in saline aquifers.[26,27] It is well-known in the petroleum industry that compositional simulations are more computationally expensive than traditional "black-oil" simulations (i.e., where the liquid hydrocarbon phase is treated as if it has only two components—oil and gas—with a simple, pressure-dependent solubility law of the gas in the liquid phase). Therefore, when reservoir fluids can reasonably be lumped into three components—oil, gas, and water—black-oil flow simulators have been used for modeling fluid flow in petroleum reservoirs. In such simulators, these three components can be partitioned into three phases, also called oil, gas, and water. In such a representation, the gas component is usually partitioned between the oil and gas phases, while the oil and water components

(17) *ECLIPSE 100: Technical Description* Schlumberger GeoQuest: 2004.
(18) Leonenko, Y.; Keith, D. W. *Environ. Sci. Technol.* **2008**, *42* (8), 2742–2747.
(19) van der Meer, L. G. H. *Energy Convers. Manage.* **1992**, *33* (5−8), 611–618.
(20) van der Meer, L. G. H. *Energy Convers. Manage.* **1993**, *34* (9−11), 959–966.
(21) van der Meer, L. G. H. *Energy Convers. Manage.* **1995**, *36* (6−9), 513–518.
(22) van der Meer, L. G. H. *Energy Convers. Manage.* **1996**, *37* (6−8), 1155–1160.
(23) Holt, T.; Jensen, J.; Lindeberg, E. *Energy Convers. Manage.* **1995**, *36* (6−9), 535–538.
(24) Law, D. H. S.; Bachu, S. *Energy Convers. Manage.* **1996**, *37* (6−8), 1167–1174.
(25) Ennis-King, J.; Gibson-Poole, C. M., Lang, S. C., Paterson, L. Long-term numerical simulation of geological storage of CO_2 in the Petrel Subbasin, North West Australia. In *Greenhouse Gas Control Technologies, Proceedings of the 6th International Conference on Greenhouse Gas Control Technologies*, Oct. 1−4, 2002, Kyoto, Japan; Gale, J., Kaya, Y. Eds.; Elsevier Science: 2003; Addendum, pp 11−16.
(26) Pruess, K.; Garcia, J., Kovscek; T., Oldenburg, C.; Rutqvist, J.; Steefel, C.; Xu, T. *Report No. 51813: Intercomparison of Numerical Simulation Codes for Geologic Disposal of CO_2*; Lawrence Berkeley National Laboratory:Berkeley, CA, 2002.
(27) Pruess, K.; Garcia, J.; Kovscek, T.; Oldenburg, C.; Rutqvist, J.; Steefel, C.; Xu, T. *Energy.* **2004**, *29* (9−10), 1431–1444.
(28) Flett, M.; Gurton, R.; Weir, G. *J. Petrol. Sci. Eng.* **2007**, *57*, 106–118.
(29) Keith, D. W.; Hassanzadeh, H.; Pooladi-Darvish, M. Reservoir engineering to accelerate dissolution of stored CO_2 in brines. In *Proceedings of 7th International Conference on Greenhouse Gas Control Technologies*, 2004; IEA Greenhouse Gas Program: Cheltenham, UK, 2005.
(30) Leonenko, Y.; Keith, D., Pooladi-Darvish, M.; Hassanzadeh, H. Accelerating the dissolution of CO_2 in aquifers. *GHGT-8, 8th International Conference on Greenhouse Gas Control Technologies*, Trondheim, Norway, 2006.

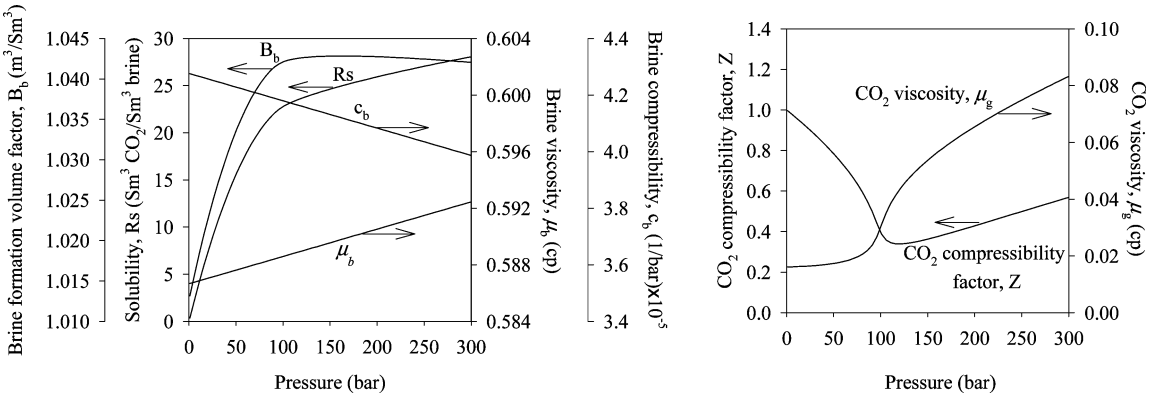

Figure 1. Brine (left) and CO_2 (right) black-oil PVT and transport properties used in numerical simulations.

generally exist only in their respective phases.[31] On the other hand, compositional models have been developed to simulate the more complex phase equilibrium systems such as those in miscible gas injection, when partitioning of a larger number of components is mechanistically important.[32] In an isothermal multicomponent system, partitioning of each component depends on pressure, the particular reservoir temperature, and the phase equilibrium properties of all components. However, for a two-component CO_2−brine system, accurate PVT (pressure-volume-temperature) calculations can be achieved using standard black-oil PVT tables, functionally dependent only on pressure. The phase equilibrium calculations in black-oil models are very fast and are simplified by table look-up of black-oil input data. This leads to much reduced computational time requirements as compared to compositional calculations requiring frequent equations of state phase equilibrium calculations. [33] The black-oil approach for simulation of CO_2 injection in saline aquifers has been reported in the literature.[22,33,34] Such black-oil representation of PVT data has been validated with experimental data[33] and successfully applied for simulation of CO_2 storage in deep saline aquifers.[22,33,34] This is an appropriate approach for most scenarios of geological storage of CO_2, where the aquifer depth is more than ~800 m and the pressure and temperature conditions are above the CO_2 critical point. However, if subsurface conditions lead to formation of a new phase or where the CO_2 is at near critical conditions, then the black-oil approach would be inappropriate.

To facilitate the usage of a black-oil simulator for CO_2 storage simulation, one needs to represent brine and CO_2 by oil and gas, respectively. The CO_2 solubility in brine can be represented by gas dissolution in oil using a solution gas−oil ratio function readily available in a black-oil simulator. In addition, shrinkage and swelling of the brine due to CO_2 evolution and dissolution can be represented by appropriate adaptation of the oil formation volume factor function in a black-oil simulator. Therefore, the requisite PVT data include gas−oil ratio (R_s) and formation volume factor (B_b) as functions of pressure. Brine and CO_2 viscosity (μ_b, μ_g), brine compressibility (c_b), and gas compressibility factor (Z) are also needed as input data. The details of converting compositional phase equilibrium data for a brine−CO_2 mixture into black-oil PVT data and estimating transport properties are given by Hassanzadeh et al.[33] The brine and CO_2 black-oil PVT properties at 50 °C used in this study are given in Figure 1.

4. Model Description

Large-scale 3D simulations of CO_2 storage are computationally expensive. On the other hand, low-resolution 3D simulations are prone to numerical errors. One alternative to simulate the storage process around an injection well is to use a relatively high-resolution 2D radial model. Although simulation results of the 2D radial models might differ from actual 3D high-resolution models, we have found that, for the problem we investigate here, the differences are smaller than those when using low-resolution 3D models.

All simulations presented here use a two-dimensional radial (r, z) model shown in Figure 2, with a permeability of 200 mD, a porosity of 25%, and a net aquifer thickness of 100 m (see Table 1 for a full list of reservoir properties). The aquifer temperature is assumed to be 50 °C, corresponding to the typical aquifers temperature in the Alberta basin.[35] The Corey exponents in the saturation functions characterize the shape of the relative permeability curves.[36] We used Corey exponents of 2 and 4 for the gas and water relative permeability curves, respectively. The relative permeability curves are assumed to be the same for imbibition and drainage. Nevertheless, one can use different relative permeability curves for the imbibition and drainage processes to study the residual gas trapping mechanism.

The completion scheme used for the brine injection well is unusual in the petroleum industry; it is used to demonstrate the effect of brine injection on CO_2 dissolution. A fully penetrated vertical brine production well is completed 20 km away from the CO_2 injection well. The well block transmisibilities for the brine injection and production wells are modified to account for the 3D effect on the well inflow performance. In the following section, the effect of aquifer size and grid block sizes are studied, and then results for the base case are presented.

5. Grid Sensitivity Studies to Study Effect of Grid Size

The common approach is to refine the grid blocks using different level of refinements. The effect of discretization on solution accuracy was investigated by conducting simulations

(31) Aziz, K.; Settari, A. *Petroleum Reservoir Simulation*; Elsevier Applied Science Publishers: London 1979.
(32) Kazemi, H.; Vestal, C. R.; Shank, G. D. *Soc. Pet. Eng. J.* **1978**, 355.
(33) Hassanzadeh, H.; Pooladi-Darvish, M.; Elsharkawy, A. M.; Keith, D. W.; Leonenko, Y. M. *Int. J. Greenhouse Gas Control.* **2008**, *2* (1), 65–77.
(34) Korbøl, R.; Kaddour, A. *Energy Convers. Manage.* **1995**, *36* (6−9), 509–512.
(35) Bachu, S.; Adams, J. J.; Michael, K.; Buschkuehle, B. E. Acid gas injection in the Alberta basin: a commercial-scale analogue for CO_2 geological sequestration in sedimentary basins. In *Proceedings of the Second Annual Conference on Carbon Dioxide Sequestration*, Alexandria, VA, May 5−8, 2003.
(36) Honarpour, M.; Koederitz, L. F.; Harvey, H. A. E. *J. Pet. Technol.* **1982**, *34*, 2905–2908.

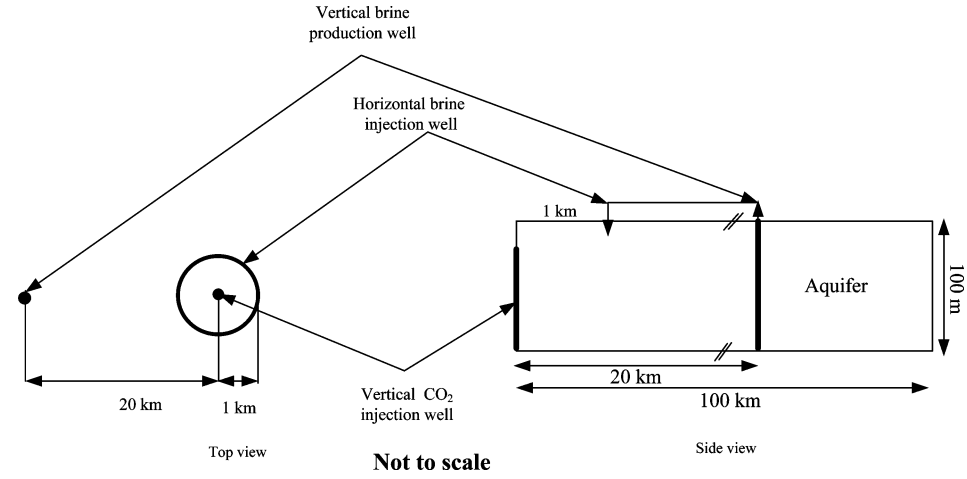

Figure 2. Top (left) and side (right) views of the aquifer and wells arrangement.

Table 1. Aquifer Properties Used in Flow Simulations

property	value
aquifer radius (km)	100
net thickness (m)	100
permeability (mD)	200
porosity (%)	25
depth (m)	1500
rock compressibility (1/bar)	1.45×10^{-5}
initial pressure (bar)	150
temperature (°C)	50
salinity (mg/L)	40000
Corey exponents for gas	2
Corey exponents for water	4

with 90 × 40, 186 × 80, and 330 × 160 grid block systems. The numerical grids in the radial direction are refined close to the wellbore, and refinement is decreased (i.e., grid sizes are increased) gradually toward the aquifer outer boundary. The grid blocks in the vertical direction are also refined at the top of the aquifer to more accurately capture the CO_2−brine displacement front. CO_2 is injected at a rate of 1 Mt/y (a typical injection rate per well in geological storage[26,27]) for 30 years into a vertical well located at the center of the domain, which is completed in the lower 80 m of the aquifer. The brine injection well is located 1 km from the center; it is completed in the top 3 m of the aquifer, and the brine injection rate is 2.81 Mt/y (7500 m^3/d). Brine injection and production starts from the beginning of CO_2 injection and continues for 200 years. Figure 3 shows the effect of grid size on bottom hole pressure of the CO_2 injection well (right) and the corresponding CO_2 dissolution (left) for three different grid block resolutions. As shown in Figure 3, the 90 × 40 resolution is not sufficiently accurate, while the 186 × 80 produces results within 1% of the 330 × 160 resolution, indicating that discretization errors become negligible at or above the 186 × 80 resolution. The sensitivity of the result to the location of the aquifer outer boundary was examined by simulating different aquifer sizes. Simulations (not shown here) show that results are not sensitive to the location of the outer boundary larger than 100 km. Therefore, the outer boundary of the aquifer of 100 km is adopted in all simulations presented herein to approximate an infinite aquifer.

6. Base Case Results and Observations

As suggested by the above grid sensitivity results, we chose a discretization of 186 × 80 ($r \times z$) as a base case and explored the possibility of increasing the rate of CO_2 dissolution by injecting brine into a radial well located 1 km distant from the central CO_2 injection well (see Figure 2). Similar to the injection scenario described in the grid sensitivity studies section, CO_2 is injected at a rate of 1 Mt/y for 30 y into a vertical well located at the center of the domain, which is completed in the lower 80 m of the aquifer. Brine injection and production at a rate of 2.81 Mt/y (7500 m^3/D) starts from the beginning of CO_2 injection and continues for 200 y. Results presented in Figure 3 (left) show the dissolution of CO_2 in formation brine with and without brine injection. Without brine injection, only 8% of the injected CO_2 dissolves in formation brine. Results presented in Figure 3 demonstrate that more than 50% of the injected CO_2 dissolves by injecting brine on top of the injected CO_2.

Figure 4 (two right-hand-side plates) shows 2D cross sections of CO_2 mobile phase saturation and CO_2 dissolved in formation brine at different times for a case with brine injection and production. The corresponding results for a case without brine injection and production are also shown in Figure 4 (two left-hand-side plates) for comparison. CO_2 dissolution efficiencies in these two scenarios are as noted above.

The rate at which injected CO_2 comes in contact with undersaturated brine ultimately limits the rate of dissolution. The injected CO_2, which is more buoyant than the formation brine, flows outward and then migrates upward. During this migration, CO_2 dissolves in the formation brine and the formation brine becomes saturated with CO_2. This period appears as a downturn in the early part of the dissolution curve as shown in Figure 3. In fact, the decreasing trend in the dissolution curve demonstrates that the formation brine in the vicinity of the injection point becomes saturated with CO_2. The minimum dissolution observed in the dissolution curve shows that the CO_2 front reaches the brine injection location. Throughout the first five years of upward CO_2 migration, two-phase flow displacement controls the dissolution process. The migration length-scale for two-phase flow in this period is usually small compared to the areal extent of the aquifer. Therefore, during the first five years of the CO_2 injection period, fractional flow of CO_2 controls the amount of CO_2 dissolved in the formation brine.

After five years of CO_2 injection, the injected CO_2 front reaches the brine injection well (located 1 km away from the center in the base case simulation). The CO_2 plume is then trapped between the CO_2 injection and the brine injection wells. A bank of fresh injected brine is gradually formed around the brine injection well. During this period, the injected CO_2 dissolves in brine in two ways. First, the downward expansion of the trapped CO_2 due to a pressure barrier at the brine injection

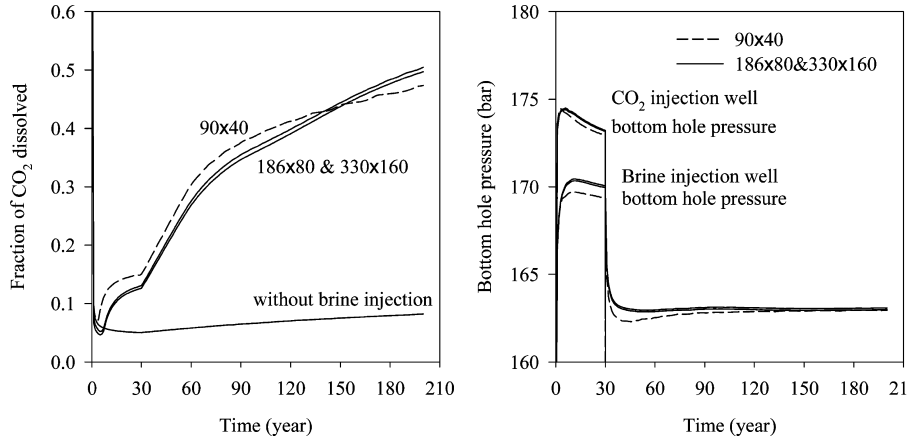

Figure 3. Grid sensitivity effect on bottom hole pressure of the CO_2 injection well (right) and CO_2 dissolution (left) for three different grid block resolutions. In all cases, 1 Mt/y of CO_2 is injected into the aquifer from the model center, and the brine injection well is located at 1 km distant with an injection rate of 2.81 Mt/y.

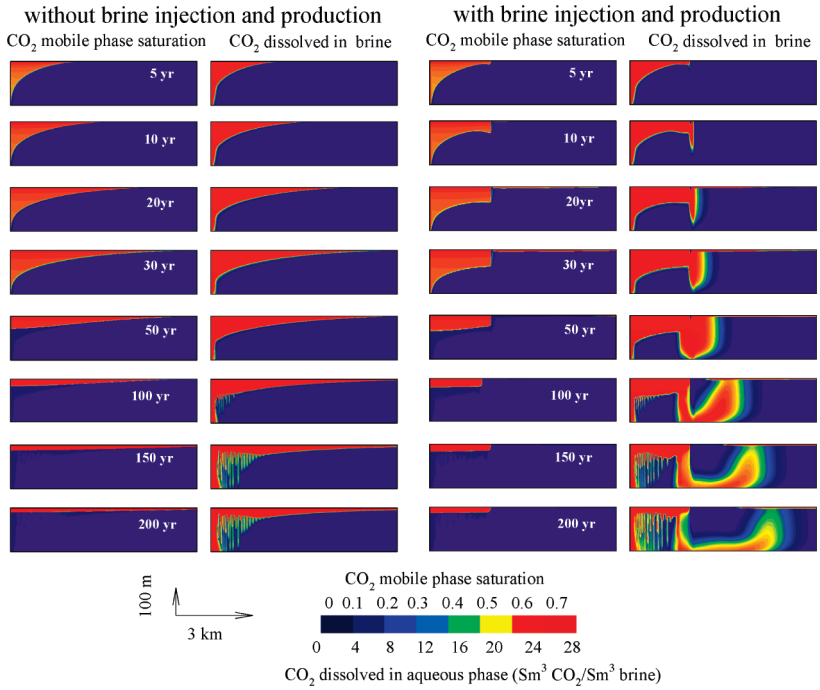

Figure 4. 2D cross-section of distribution of CO_2 mobile phase and CO_2 dissolved in formation brine for different times and for two cases of without (left plates) and with (right plates) brine injection and production. The vertical axis is aquifer height (100m) and the horizontal axis is aquifer radius (shown to a maximum of 3 km). In the case with brine injection and production, the brine injection well is located at 1 km distant from the model center with a brine injection and production rate of 2.81 Mt/y. In both cases, 1 Mt/y CO_2 is injected into the aquifer via a vertical well located at the model center.

well brings the injected CO_2 in contact with the injected brine and causes some dissolution. Second, a fraction of the CO_2 migrates upward, flowing radially through, and dissolving into, the fresh bank of injected brine. If the rate of the injected brine is not sufficient to dissolve all of the migrating CO_2, then a fraction of the mobile CO_2 phase leaks radially through the brine plume. During this period, the two-phase flow displacement and vertical permeability control the shape of the dissolution curve.

At time-scales longer than a few decades, density-driven flow within the brine eventually becomes an important mechanism for accelerating dissolution by increasing mass transfer. Density differences arise because the CO_2-saturated brine is slightly denser than the fresh formation brine. Density-driven flow or free convective mixing can potentially dissolve a large fraction of injected CO_2 in formation brines in an extended period of time. For the case studied, the free convective mixing due to such density differences contributes to dissolving CO_2 after 100 y of simulation. During and shortly after the CO_2 injection period, where the dominant mechanism is two-phase flow displacement, resolving the fingering effect (convection) requires high spatial resolution. Low spatial resolution may cause an overestimation of dissolution due to numerical smearing (numerical diffusion) at the CO_2 front. With longer time scales, where the density-driven flow becomes important, a lower spatial resolution may underestimate dissolution because the numerical diffusion may reduce the density contrast, thereby reducing the convective instability. Such behavior is observed for a case where simulation grid blocks were coarse (90×40) as shown in Figure 3 (left). The coarse grid block simulation (90×40) in Figure 3 (left) demonstrates higher dissolution at early times but underestimates dissolution over longer periods of time once the density fingering evolves. In the following section, we investigate the effect of parameters such as aquifer

Table 2. Effect of Aquifer Parameters on CO_2 Dissolution in Formation Brine after 30 y (End of the CO_2 Injection Period) and 200 y (End of the Brine Injection and Production Period)

aquifer parameters	variations	dissolution (%) 30 y	dissolution (%) 200 y
formation thickness (m)	25, 50, 75, 100	15.8, 14.3, 13.5, 13.1	45.2, 49.8, 51.2, 50.5
tilt angle	0°, 1°	13.1, 13.0	50.5, 51.9
formation anisotropy	0.01, 0.10, 1.0	14.6, 13.6, 13.1	66.2, 44.9, 50.5
layering	no layering, three layers	13.1, 14.4	50.5, 54.5

layering, formation thickness, tilt angle, and permeability anisotropy on the solubility trapping of CO_2 in brine formations.

7. Effect of Aquifer Properties

Simulations were conducted to investigate the effect of some aquifer properties on the dissolution of the injected CO_2 into the aquifer brine. In all cases, the rates of CO_2 injection and brine injection and production were similar to the base case. Dissolution results at the end of CO_2 injection at 30 y and also at the end of brine injection and production at 200 y are presented in Table 2. The lesser formation thickness shows higher dissolution during the CO_2 injection period due to more efficient contact between CO_2 and the injected brine. On the other hand, after CO_2 injection stops, the lesser formation thickness leads to less override and therefore a smaller contact area, resulting in less dissolution. After CO_2 injection stops, the velocity of the injected brine that removes CO_2 from the mixing zone affects the mixing process to a small degree as is shown for two thickness cases of 75 and 100 m. It is also observed that cases with greater formation thicknesses demonstrate greater fingering instabilities at long times. Simulations were also performed to investigate the role of aquifer tilt angle. Results presented in Table 2 reveal that a 1° tilt angle leads to slightly higher dissolution.

Simulations were also performed to investigate the effect of vertical permeability anisotropy ratio ($\gamma = k_V/k_H$) on dissolution. Figure 5 demonstrates that CO_2 solubility is not a monotonic function of formation vertical permeability anisotropy. This can be explained by considering competition between convective mixing, downward expansion of the CO_2 free phase plume created by the pressure barrier at the brine injection well, and vertical migration of CO_2 through the fresh brine. Results presented in Figure 5 also reveal that, with the very low vertical anisotropy ratio of 0.01, the prevailing mechanism is downward expansion of the injected CO_2, resulting in significantly higher dissolution. For an anisotropy ratio equal to unity, upward migration is dominant; therefore, migrated CO_2 flows through the bank of the fresh injected brine on top of the aquifer. For an anisotropy ratio of 0.1, both mechanisms of downward expansion and vertical migration are acting concurrently, but to an overall lesser degree, leading to lower dissolution. For anisotropy ratios of 0.01 and 0.1, free convective mixing, which is affected by vertical permeability, was not observed.

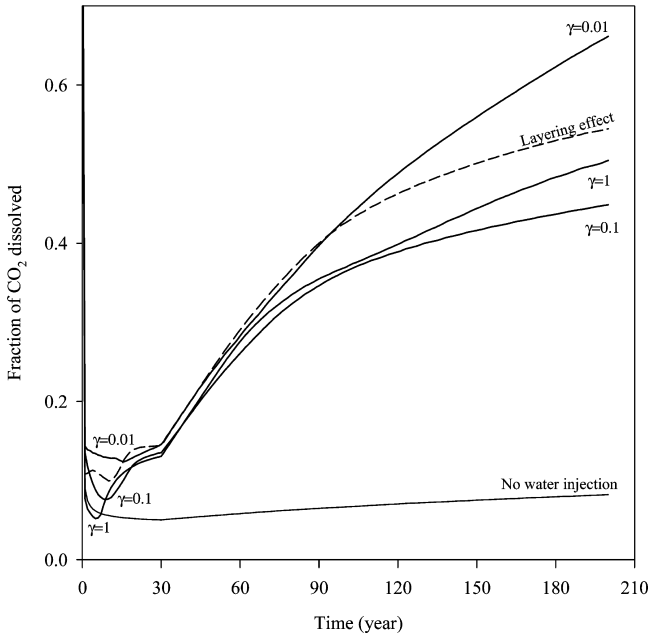

Figure 5. Effect permeability anisotropy and layering on dissolution.

A simulation case was also carried out by including three layers of shale of 2 mD sandwiched between sand layers of 200 mD, similar to layering used by Preuss et al.[27] The effect of shale layers is to retard migration of CO_2 to the top of the aquifer by splitting the CO_2 mobile phase front depending on the number of shale layers. Splitting the migrated CO_2 into several fronts enhances the solubility trapping mechanism as shown in Figure 5, resulting from increasing the contact area between CO_2 and fresh brine.

8. Engineering Analysis

An engineering study was performed to construct an estimate of the energy costs of brine injection and production based on injection of 1 Mt/y of CO_2 for 30 y. In all cases, brine is injected for 200 y on top of the CO_2 plume by an injection well 1 km distant from the CO_2 injection site and is produced for 200 y by a production well 20 km distant from the CO_2 injection site.

We first investigated the effect of altering the radial position of the brine injection well. For an injection rate of 2.81 Mt/y, dissolution is maximized by placing the injection well at a radius of approximately 1 km (Figure 6, right). For these simulations, it was necessary to refine the grid resolution in the vicinity of the brine injection well to a minimum grid size of 4 m. During the 30 y CO_2 injection period, a brine injection well close to the CO_2 injection well at the model center leads to higher dissolution rates. However, the brine in the vicinity of the CO_2 injection well becomes saturated with CO_2, leading to most of the injected CO_2 passing the brine injection well without any further dissolution. As the brine injection well distance from the model center increases, the CO_2 front takes longer to reach the brine injection well, leading to lower dissolution rates during CO_2 injection. After CO_2 injection stops, a brine injection well located far from the center demonstrates higher dissolution, since the contact area between CO_2 and brine increases with the square of well radius. By further increasing the brine injection well distance—for instance to 1.5 km—the CO_2 front does not reach the brine injection well in the time frame studied, demonstrating a lower dissolution.

We then investigated the effect of varying brine injection and production rates while fixing the brine injection well radius at 1 km. Solubility of CO_2 in brine at the aquifer salinity and temperature is about 0.045 (kg/kg). A zero order approximation, would suggest that approximately 670 Mt of brine is needed to dissolve all of the injected CO_2. This zero-order calculation assumes complete mixing between the injected brine and the CO_2 and ignores the fraction of injected CO_2 that dissolves in the in situ brine. In this study we numerically investigated the fraction of the CO_2 that would be dissolved, when the injected brine ranges between

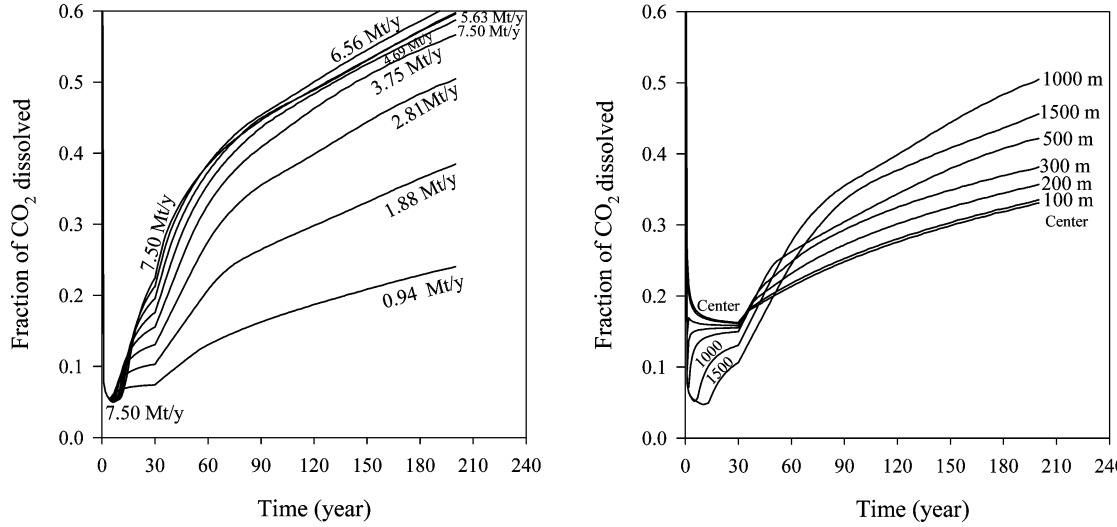

Figure 6. Effect of brine injection well location on dissolution for 2.81 Mt/y of brine injection and production (right) and effect of brine injection and production rate on dissolution at optimum brine injection well location of 1 km from the center (left).

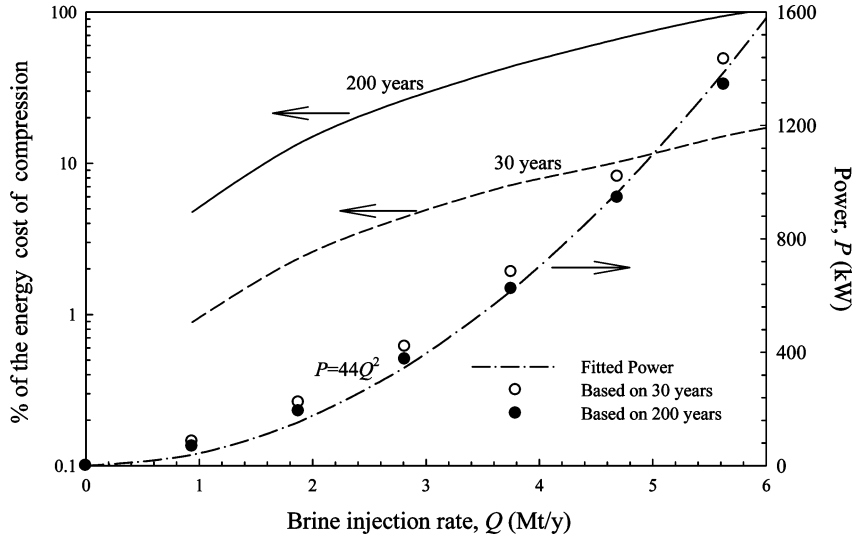

Figure 7. Power needed to run the brine injection/production pumps as a function of brine injection/production rate for two scenarios of 30 and 200 y brine injection/production and different cost ratios as a function of brine injection/production rate for 30 and 200 y of brine injection/production.

approximately 1 and 8 times this values. As seen in Figure 6 (left), the dissolved CO_2 fraction generally increases with brine injection and production rate. However, the results indicate that the dissolved CO_2 fraction increases relatively slowly as injection and production rates are increased beyond about 3 Mt/y. Results presented in Figure 6 (left) show that by further increasing the brine injection and production rate, dissolution decreases slightly. This results from the fact that, due to higher injection pressures resulting from very high brine injection rates, the amount of CO_2 trapped as free-phase CO_2 between the two injection wells is higher as compared to that of lower brine injection rates. Therefore, dissolution ultimately decreases by increasing the brine injection rate. For such cases with high brine injection rates, less density fingering was also observed that might have contributed to slightly lower dissolution.

We assume that the energy cost of this scheme is dominated by the energy cost required to run the injection/production pumps. For a 2.4 Mt/y brine injection/production rate, for example, the required power may be estimated at 240 kW, which would have an undiscounted cost of $15 million over 200 years at an electricity cost of 5 c/kWh, while the cost is reduced to $1.5 million at an economic discount rate of 5%.

The energy cost of brine injection/production is estimated based on the time-integrated total work for various rates of brine injection/production and 1 Mt/y CO_2 injected as shown in Figure 7. As a convenient metric, we compare the energy required for brine injection/production to the energy required for of CO_2 compression from atmospheric pressure to reservoir conditions, which we approximate as 300 kJ/kg of CO_2. This allows a simple order-of-magnitude comparison of the energy costs of brine injection/production compared to the costs of CO_2 capture. The energy cost for CO_2 compression is typically a small fraction (10−30%) of the energy penalty associated with CO_2 capture.

Figure 7 shows the average power required to run the brine injection/production pumps versus brine injection/production rate. Results show that power increases as the square of the injection rate, as expected. In Figure 8, the amount of dissolution achieved is plotted as a function of the brine injection energy, which is in turn expressed with respect to the energy that would be required for CO_2 compression. At

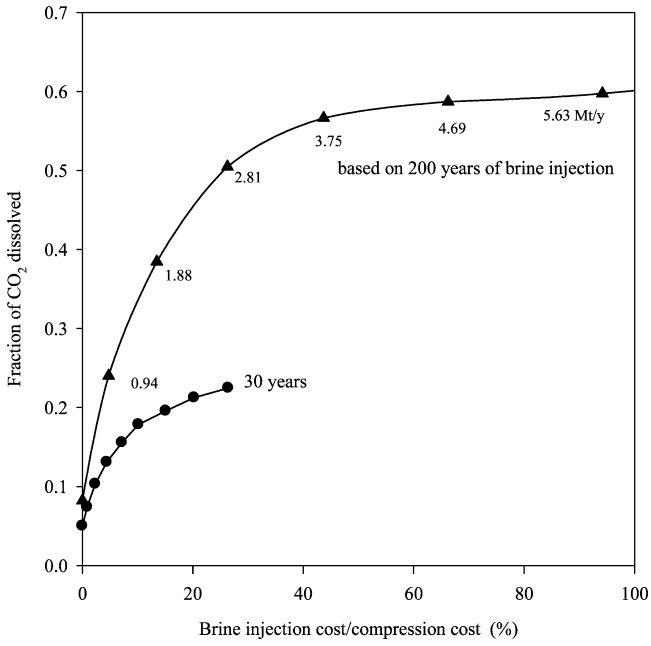

Figure 8. Dissolution of CO_2 in formation brine as a function of brine injection to CO_2 compression cost ratio for two scenarios of 30 and 200 y brine injection/production. The numbers on the curve show Mt/y of brine injected into the aquifer.

a brine injection to CO_2 compression energy cost ratio of 20%, for example, the ultimate CO_2 dissolutions after 30 and 200 y are 22 and 45%, respectively. From Figure 7, the corresponding brine injection/production rate to reach 45% dissolution is about 2.4 Mt/y. Therefore, running the brine injector/producer for 30 and 200 y results in dissolution increases of 14 and 23%, respectively. Since we compare the dissolution increase of cases with and without brine injection/production, it is worth mentioning that the extra pressure increase caused by 2.4 Mt/y brine injection on the CO_2 injection well is roughly 10 bar. The corresponding power for this pressure increase is negligible as compared to the total compression cost of CO_2.

9. Discussion and Conclusions

We present a method for accelerating CO_2 dissolution in saline aquifers by injecting brine on top of the injected CO_2. Simulation studies for idealized aquifer geometry are presented here to investigate the fate of injected CO_2 in a relatively short period of time after CO_2 injection has ceased. We have experimented with injection of 1 Mt/y of CO_2 in a saline aquifer for a 30 y period, a duration consistent with the average life of a power plant, and study the role of brine injection on top of the injected CO_2. Effects of a number of reservoir engineering parameters are investigated. Results reveal that formation anisotropy, layering, and formation thickness have important bearing on the CO_2 dissolution process. It is shown that, without brine injection, only a small fraction (less than 8%) of the injected CO_2 would be trapped by dissolving in formation brine within 200 y. For the particular acceleration case studied, however, more than 50% of the injected CO_2 dissolves in the aquifer as induced by brine injection.

It may be possible to engineer CO_2 storage in deep saline aquifers by accelerating the dissolution of CO_2 in brines in order to reduce the long-term risk of leakage. Such reservoir engineering techniques include: (i) optimizing the geometry of brine injection wells to maximize the rate at which buoyancy-driven flow of CO_2 and brines drive dissolution, and (ii) use of wells and pumps to transport CO_2 or brines within the reservoir in order to increase contact between CO_2 and undersaturated brines, thereby accelerating the rate of dissolution. Such reservoir engineering techniques can be used to accelerate the reduction of free CO_2 phase saturations, thereby decreasing the risk of CO_2 leakage in the short term—that is, before the long-term processes of diffusion, free convective mixing, and mineral immobilization become effective.

Analysis presented in this work is a preliminary engineering and economic assessment for using brine injection to accelerate CO_2 dissolution in aquifers. The well geometry in this study was chosen to create a large contact area between the injected water and the CO_2 in the reservoir. To accommodate requirements of a radial model, we chose a circular horizontal well. In practice, this may be replaced by a ring of vertical injectors or four horizontal injectors forming a square. The time of water injection in this study was 200 y. This time frame is not common in petroleum industry (for example in oil recovery projects). Parameters including injection well geometry, injection time, distance between injector and producer are design parameters that will need to be selected on a case-by-case basis. In the simulations presented, the saline formation was assumed homogeneous, a hypothesis that will definitely not be valid for most real geological formations. Permeability heterogeneity might have a large impact on the CO_2−brine displacement in saline aquifers. For example, the permeability variations resulted from various degree of shale content influence the vertical and lateral displacement and subsequent migration. Therefore, we speculate that, in such cases the dissolution of CO_2 in brine will likely be different from what has been obtained in this analysis. The scale of permeability variation is also an important factor that might control the long-term migration of CO_2 in geological formations. Similar studies based on large-scale geological models populated by more realistic permeability and porosity fields would be required on a case-by-case basis. In addition, an ideal geometry for brine injection was used to demonstrate the effect of brine injection on CO_2 dissolution. Nevertheless, using current multilateral well drilling technology this idealized geometry can be closely implemented in real field scale applications. Further investigations based on more realistic well pattern and reservoir geometries are needed. Nevertheless, preliminary results demonstrated potential for acceleration CO_2 dissolution in formation brine and reducing risk of leakage of CO_2 from storage sites at relatively low cost. Subsequent to the completion of this work, Leonenko and Keith[18] have recently demonstrated that geometry of the aquifer could further affect rate of dissolution, leading to promising application of the brine injection scheme developed here for accelerating CO_2 dissolution.

Acknowledgment. The financial support for this work was provided by Alberta Energy Research Institute (AERI), Alberta DOE, and NSERC. Simulation software (Eclipse 100) was donated by Schlumberger (GeoQuest). These supports are gratefully acknowledged.

Nomenclature

B_b = formation volume factor, m^3 of brine at reservoir condition/m^3 of brine at SC
c_b = brine compressibility, 1/bar
IPCC = Intergovernmental Panel on Climate Change
k_H = horizontal permeability, mD

k_{rg} = gas-phase relative permeability, dimensionless
k_{rw} = brine relative permeability, dimensionless
k_V = vertical permeability, mD
mD = milliDarcy
Mt = mega-ton
P = power, kW
PVT = pressure-volume-temperature
Q = brine injection or production mass flow rate (Mt/y)
r = radial coordinate, m
R_s = solution gas-oil ratio, m^3 of gas at SC /m^3 of brine at SC
z = vertical coordinate, m
Z = gas compressibility factor, dimensionless
γ = formation vertical permeability anisotropy ratio = k_V/k_H, dimensionless
μ_b = brine viscosity, cp
μ_g = gas viscosity, cp

EF900125M